Direct Voltage Control of DC-DC Boost Converters Using Model Predictive Control Based on Enumeration

Petros Karamanakos*, Tobias Geyer†, and Stefanos Manias*
* National Technical University of Athens, Athens, Greece, e-mail: petkar@central.ntua.gr, manias@central.ntua.gr
†ABB Corporate Research, Baden-Dättwil, Switzerland, e-mail: t.geyer@ieee.org

***Abstract*— This paper presents a model predictive control (MPC) approach for the dc-dc boost converter. Based on a hybrid model of the converter suitable for both continuous and discontinuous conduction mode an objective function is formulated, which is to be minimized. The proposed MPC scheme, utilized as a voltage-mode controller, achieves regulation of the output voltage to its reference, without requiring a subsequent current control loop. Simulation and experimental results are provided to demonstrate the merits of the proposed control methodology, which include fast transient response and robustness.**

***Keywords*— DC-DC converter, model predictive control, hybrid system.**

I. Introduction

Over the past decades dc-dc conversion has matured into a ubiquitous technology, which is used in a wide variety of applications, including dc power supplies and dc motor drives [1]. Dc-dc converters are intrinsically difficult to control due to their switching behavior, constituting a switched non-linear or *hybrid* system. To date, a plethora of control schemes has been proposed to address these difficulties.

Although existing control approaches have been shown to be reasonably effective, several challenges have not been fully addressed yet, such as ease of controller design and tuning, as well as robustness to load parameter variations. Furthermore, the computational power available today and the recent theoretical advances with regards to controlling hybrid systems allow one to tackle these problems in a novel way. The aim is not only to improve the performance of the closed-loop system, but to also enable a systematic design and implementation procedure. Model predictive control (MPC) is a particularly promising candidate to achieve this [2], since it allows one to directly include constraints in the design phase and to address the switching or hybrid nature of dc-dc converters. MPC was developed in the 1970s in the process control industry, and has recently been introduced to the field of power electronics. This includes three-phase dc-ac and ac-dc systems such as [3]–[5], as well as dc-dc converters [6]–[11].

In MPC the control action is obtained by solving online at each time-step an optimization problem with a given objective function over a finite prediction horizon, subject to the discrete-time model of the system. The optimal sequence of control inputs is the one that minimizes the objective function and thus yields the best predicted performance of the system. To provide feedback, allowing one to cope with model uncertainties and disturbances, only the first input of the sequence is applied to the converter. At the next time-step, the optimization problem is repeated with new measurements or estimates. This procedure is known as the *receding horizon policy* [12], [13].

In this paper, MPC is employed as a voltage-mode controller for the dc-dc boost converter. The main control objective is the regulation of the output voltage to a commanded value, while rejecting variations in the input voltage and the load. The discrete-time model of the converter used by the controller is designed such that it accurately predicts the plant behavior both when operating in continuous (CCM) as well as in discontinuous conduction mode (DCM). As a result, the formulated controller is applicable to the whole operating regime, rather than just a particular operating point. To address time-varying and unknown loads, a Kalman filter is added that estimates the converter states and provides offset-free tracking of the output voltage due to its integrating action, despite changes in the load. In that way the robustness of the controller is ensured even when the converter operates under non-nominal conditions.

The proposed scheme carries several benefits. The very fast dynamics achieved by MPC, combined with its inherent robustness properties, are some of its key beneficial characteristics. Furthermore, thanks to the fact that the control objectives are expressed in the objective function in a straightforward manner, the design process is simple and laborious tuning is avoided. The inherent computational complexity is the most prominent drawback—the computational power required increases exponentially as the prediction horizon is extended. Moreover, the absence of a modulator and the direct manipulation of the converter switches imply a variable switching frequency.

This paper is organized as follows. In Section II the hybrid continuous-time model of the converter, suitable for both CCM and DCM, is presented. Furthermore, the discrete-time model that will be used as the prediction model is derived. The control objectives are summarized in Section III, and the MPC problem is formulated and solved in Section IV. Section V presents simulation re-

978-1-4673-1972-0/12/$31.00 ©2012 IEEE

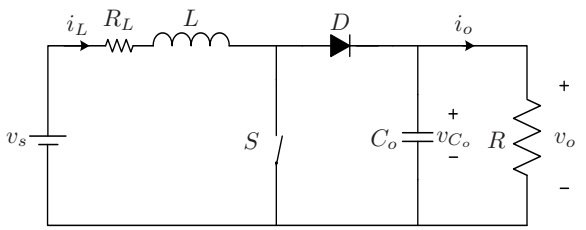

Fig. 1: Topology of the dc-dc boost converter.

sults illustrating the performance of the proposed control approach. In Section VI the experimental validation of the introduced strategy is provided. The paper is summarized in Section VII, where conclusions are drawn.

II. Physical Model of the Boost Converter

A. Continuous-Time Model

The dc-dc boost converter shown in Fig. 1 is a converter that increases the dc input voltage $v_s(t)$ to a higher dc output voltage $v_o(t)$. The converter consists of two power semiconductors—the controllable switch S, and the passive switch D. A low pass filter is added, consisting of the inductor L with the internal resistor R_L, and the capacitor C_o.

Associated with the switch positions are three different non-linear dynamics. When the switch is *on* ($S = 1$), energy is stored in the inductor L and the inductor current $i_L(t)$ increases. When the switch is *off* ($S = 0$), the inductor is connected to the output and energy is released through it to the load, resulting in a decreasing $i_L(t)$. Furthermore, when the switch S remains *off* and $i_L(t) = 0$, then both S and D are *off* and the output voltage drains into the load. In this case, the converter operates in DCM.

The state-space representation of the converter in the continuous-time domain is given by the following equations [14]

$$\frac{dx(t)}{dt} = \big(A_1 + A_2 u(t)\big)x(t) + B v_s(t) \tag{1a}$$

$$y(t) = Cx(t)\,, \tag{1b}$$

where

$$x(t) = [i_L(t)\ v_o(t)]^T \tag{2}$$

is the state vector, encompassing the inductor current and the output voltage across the output capacitor. The system matrices are given by

$$A_1 = \begin{bmatrix} -\frac{d_{aux}R_L}{L} & -\frac{d_{aux}}{L} \\ \frac{d_{aux}}{C_o} & -\frac{1}{C_o R} \end{bmatrix}, \quad A_2 = \begin{bmatrix} 0 & \frac{d_{aux}}{L} \\ -\frac{d_{aux}}{C_o} & 0 \end{bmatrix},$$

$$B = [\frac{d_{aux}}{L}\ 0]^T, \quad \text{and} \quad C = [0\ 1]\,,$$

where R is the load resistance and the output $y = v_o(t)$ is the output voltage. The variable u denotes the switch position, with $u = 1$ implying that the switch S is *on*, and $u = 0$ referring to the case where the switch S is *off*. Finally, d_{aux} is an auxiliary binary variable [15] that is $d_{aux} = 0$ if the converter operates in DCM (i.e. $S = 0$ and $i_L(t) \leq 0$), and $d_{aux} = 1$ if it operates in CCM, i.e. either $S = 0$ and $i_L(t) > 0$ or $S = 1$, see Fig. 2.

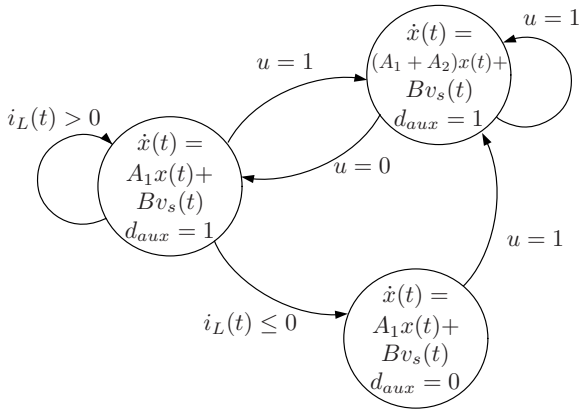

Fig. 2: Dc-dc converter presented as automaton driven by conditions.

B. Discrete-Time Model

The derivation of an adequate model of the boost converter to serve as an internal prediction model for MPC is of fundamental importance. Based on the continuous-time state-space model (1) and using the forward Euler approximation approach, the following discrete-time model of the converter is derived.

$$x(k+1) = \big(E_1 + E_2 u(k)\big)x(k) + F v_s(k) \tag{3a}$$

$$y(k) = Gx(k) \tag{3b}$$

where the matrices are $E_1 = \mathbf{1} + A_1 T_s$, $E_2 = A_2 T_s$, $F = BT_s$, and $G = C$, where $\mathbf{1}$ is the identity matrix and T_s is the sampling interval.

III. Control Problem

For the dc-dc converter, the main control objective is for the output voltage to accurately track its given reference—or equivalently to minimize the output voltage error—by appropriately manipulating the switch. This is to be achieved despite changes in the input voltage and load. During transients, the output voltage is to be regulated to its new reference value as fast and with as little overshoot as possible.

IV. Model Predictive Control

In this section an MPC scheme for dc-dc boost converters is introduced, which directly controls the output voltage by manipulating the switch S. Using an enumeration technique, the user-defined objective function is minimized subject to the converter dynamics.

A. Objective Function

The objective function is chosen as

$$J(k) = \sum_{\ell=k}^{k+N-1} \Big(|v_{o,err}(\ell+1|k)| + \lambda |\Delta u(\ell|k)| \Big) \tag{4}$$

which penalizes the absolute values of the variables of concern over the finite prediction horizon N. The first

term penalizes the absolute value of the output voltage error

$$v_{o,err}(k) = v_{o,ref} - v_o(k)\,. \tag{5}$$

By penalizing the difference between two consecutive switching states, the second term aims at decreasing the switching frequency and avoiding excessive switching

$$\Delta u(k) = u(k) - u(k-1)\,. \tag{6}$$

The weighting factor $\lambda > 0$ sets the trade-off between output voltage error and switching frequency.

B. Optimization Problem

The optimization problem underlying MPC at time-step k amounts to minimizing the objective function (4) subject to the converter model dynamics

$$\begin{aligned} &U^*(k) = \arg\min J(k) \\ &\text{subject to eq. (3)}\,. \end{aligned} \tag{7}$$

The optimization variable is the sequence of switching states over the horizon, which is $U(k) = [u(k)\ u(k+1) \dots u(k+N-1)]^T$. Minimizing (7) yields the optimal switching sequence $U^*(k)$. Out of this sequence, the first element $u^*(k)$ is applied to the converter; the procedure is repeated at $k+1$, based on new measurements acquired at the following sampling instance.

Minimizing (7) is a challenging task, since it is a mixed-integer non-linear optimization problem. A straightforward alternative is to solve (7) using enumeration, which involves the following three steps. First, by considering all possible combinations of the switching states ($u = 0$ or $u = 1$) over the prediction horizon, the set of admissible switching sequences is assembled. For each of the 2^N sequences, the corresponding output voltage trajectory is predicted and the objective function is evaluated. The optimal switching sequence is obtained by choosing the one with the smallest associated cost.

C. Move Blocking

A fundamental difficulty associated with boost converters arises when controlling their output voltage without an intermediate current control loop, since the output voltage exhibits a non-minimum phase behavior with respect to the switching action. For example, when increasing the output voltage, the duty cycle of switch S has to be ramped up, but initially the output voltage drops before increasing. This implies that the sign of the gain (from the duty cycle to the output voltage) is not always positive. To overcome this obstacle and to ensure closed-loop stability, a sufficiently long prediction interval NT_s is required, so that the controller can "see" beyond the initial voltage drop when contemplating to increase the duty cycle.

However, increasing N leads to an exponential increase in the number of switching sequences to be considered and thus dramatically increases the number of calculations needed. A long prediction interval NT_s with a small N and a small T_s can be achieved by employing a *move blocking* technique. For the first steps in the prediction horizon, the prediction model is sampled with T_s, while for steps far in the future, the model is sampled more coarsely with a multiple of T_s, i.e. n_sT_s, with $n_s \in \mathbb{N}^+$ [16]. As a result, different sampling intervals are used within the prediction horizon, as illustrated in Fig. 3. We use N_1 to denote the number of prediction steps in the first part of the horizon, which are sampled with T_s. Accordingly, N_2 refers to the number of steps in the last part of the horizon, sampled with n_sT_s. The total number of time-steps in the horizon is $N = N_1 + N_2$.

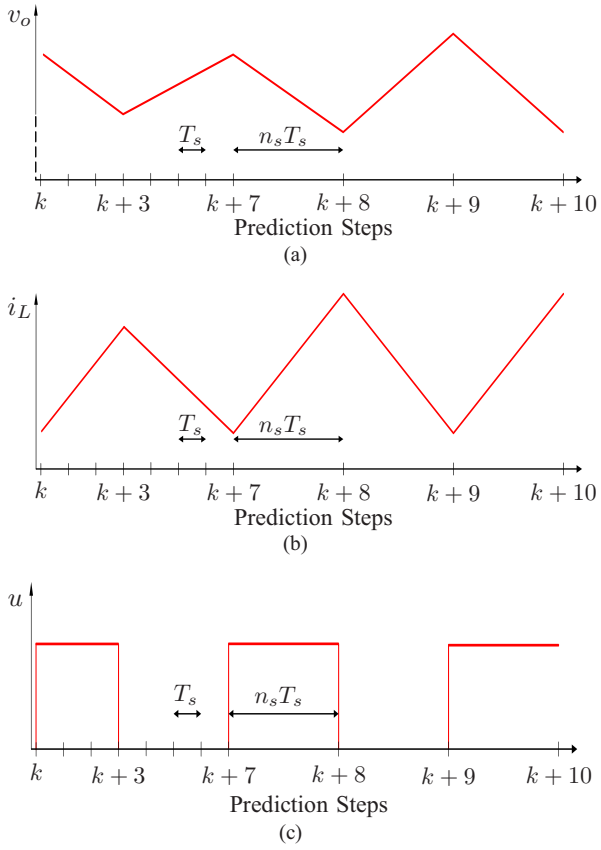

Fig. 3: Prediction horizon with move blocking: a) output voltage, b) inductor current, and c) control input. The prediction horizon has $N = 10$ time-steps, but the prediction interval is of length $19T_s$, since $n_s = 4$ is used for the last $N_2 = 3$ steps.

D. Load Uncertainty

In most applications the load is unknown and time varying. Thus, an external estimation loop should be added, which allows the elimination of the output voltage error under load uncertainties. This additional loop is employed to provide state estimates to the previously derived optimal controller, where the load was assumed to be known and constant. Furthermore, the output voltage reference is adjusted so as to compensate the deviation of the output voltage from its actual reference.

To achieve both of these goals a discrete-time Kalman filter [17] is designed similar to [8]; thanks to its integrating nature it provides a zero steady-state output voltage error. Two integrating disturbance states, i_e and v_e, are introduced in order to model the effect of the load variations on the inductor current and output voltage respectively. The measured state variables, i_L and v_o,

together with the disturbance state variables form the augmented state vector

$$x_a = [i_L \; v_o \; i_e \; v_e]^T \,. \tag{8}$$

The Kalman filter is used to estimate the state vector given by (8). Based on the switching position ($u = 0$ or $u = 1$) and the converter operating mode ($d_{aux} = 0$ or $d_{aux} = 1$) three different affine systems result; the respective stochastic discrete-time state equations of the augmented model are

$$x_a(k+1) = \xi(k) + \begin{cases} E_{1a}x_a(k) & u = 0 \;\&\; d_{aux} = 0 \\ E_{1a}x_a(k) + F_a v_s & u = 0 \;\&\; d_{aux} = 1 \\ E_{2a}x_a(k) + F_a v_s & u = 1 \;\&\; d_{aux} = 1 \end{cases} . \tag{9}$$

The measured state is given by

$$x(k) = \begin{bmatrix} i_L(k) \\ v_o(k) \end{bmatrix} = G_a x_a(k) + \nu(k) \,. \tag{10}$$

The matrices are

$$E_{1a} = \begin{bmatrix} E_1 & \mathbf{0} \\ \mathbf{0} & \mathbf{1} \end{bmatrix}, \quad E_{2a} = \begin{bmatrix} E_1 + E_2 & \mathbf{0} \\ \mathbf{0} & \mathbf{1} \end{bmatrix}, \\ F_a = \begin{bmatrix} F \\ 0 \\ 0 \end{bmatrix}, \quad \text{and} \quad G_a = \begin{bmatrix} \mathbf{1} & \mathbf{1} \end{bmatrix} \tag{11}$$

where $\mathbf{1}$ is the identity matrix of dimension two and $\mathbf{0}$ are square zero matrices of dimension two. The variables $\xi \in \mathbb{R}^4$ and $\nu \in \mathbb{R}^2$ denote the process and the measurement noise, respectively; these noise disturbances represent zero-mean, white Gaussian noise sequences with normal probability distributions. Their covariances are given by $E[\xi\xi^T] = Q$ and $E[\nu\nu^T] = R$, and are positive semi-definite and positive definite, respectively.

A switched discrete-time Kalman filter is designed based on the augmented model of the converter. The active mode of the Kalman filter (one out of three) is determined by the switching position and the operating mode of the converter.

Due to the fact that the state-update for each operating mode is different, three Kalman gains K_z, with $z = \{1, 2, 3\}$, need to be calculated. Consequently, the equation for the estimated state $\hat{x}_a(k)$ is the following:

$$\hat{x}_a(k+1) = \begin{cases} K_1 G_a\big(x_a(k) - \hat{x}_a(k)\big) \\ K_2 G_a\big(x_a(k) - \hat{x}_a(k)\big) \\ K_3 G_a\big(x_a(k) - \hat{x}_a(k)\big) \end{cases} + \\ + \begin{cases} E_{1a}\hat{x}_a(k) & u = 0 \;\&\; d_{aux} = 0 \\ E_{1a}\hat{x}_a(k) + F_a v_s & u = 0 \;\&\; d_{aux} = 1 \\ E_{2a}\hat{x}_a(k) + F_a v_s & u = 1 \;\&\; d_{aux} = 1 \end{cases} . \tag{12}$$

The noise covariance matrices Q and R are chosen such that high credibility is assigned to the measurements of the physical states (i_L and v_o), whilst low credibility is assigned to the dynamics of the disturbance states (i_e and v_e). The Kalman gains are calculated based on that matrices; the estimated disturbances, provided by the resulting filter, can be used in order to remove their influence from the output voltage. Hence, the disturbance state $\hat{v}_e$ is used to adjust the output voltage reference $v_{o,ref}$

$$\tilde{v}_{o,ref} = v_{o,ref} - \hat{v}_e \,. \tag{13}$$

Finally, the estimated states, $\hat{i}_L$ and $\hat{v}_o$, are used as inputs to the controller, instead of the measured states, i_L and v_o.

E. Control Algorithm

The proposed control concept is summarized in Algorithm 1. The function f stands for the state-update given by (3), with the subscripts 1 and 2 corresponding to the sampling interval being used, i.e. T_s and $n_s T_s$ respectively. Figure 4 depicts the block diagram of the introduced algorithm.

Algorithm 1 MPC algorithm

function $u^*(k)$ = MPC $(\hat{x}(k), u(k-1))$
  $J^*(k) = \infty$; $u^*(k) = \emptyset$; $x(k) = \hat{x}(k)$
  for all U over N **do**
    $J = 0$
    for $\ell = k$ to $k + N - 1$ **do**
      if $\ell < k + N_1$ **then**
        $x(\ell+1) = f_1(x(\ell), u(\ell))$
      else
        $x(\ell+1) = f_2(x(\ell), u(\ell))$
      end if
      $v_{o,err}(\ell+1) = \tilde{v}_{o,ref} - v_o(\ell+1)$
      $\Delta u(\ell) = u(\ell) - u(\ell-1)$
      $J = J + |v_{o,err}(\ell+1)| + \lambda|\Delta u(\ell)|$
    end for
    if $J < J^*(k)$ **then**
      $J^*(k) = J$, $u^*(k) = U(1)$
    end if
  end for
end function

V. Simulation Results

In this section simulation results are presented to demonstrate the performance of the proposed controller under several operating conditions. Specifically, the closed-loop converter behavior is examined in both CCM and DCM. The dynamic performance is investigated during start-up. Moreover, the response of the output voltage to step changes in the commanded voltage reference and in the input voltage is illustrated.

The circuit parameters are $L = 450\,\mu$H, $R_L = 0.3\,\Omega$ and $C_o = 220\,\mu$F. The load resistance is equal to $R = 73\,\Omega$ and assumed to be known to the controller. The weight in the objective function is $\lambda = 0.1$, the prediction horizon is $N = 14$ and the sampling interval is $T_s = 2.5\,\mu$s. A move blocking scheme is used with $N_1 = 8$, $N_2 = 6$ and $n_s = 4$, i.e. the sampling interval for the last six steps in the prediction interval is $T_s = 10\,\mu$s.

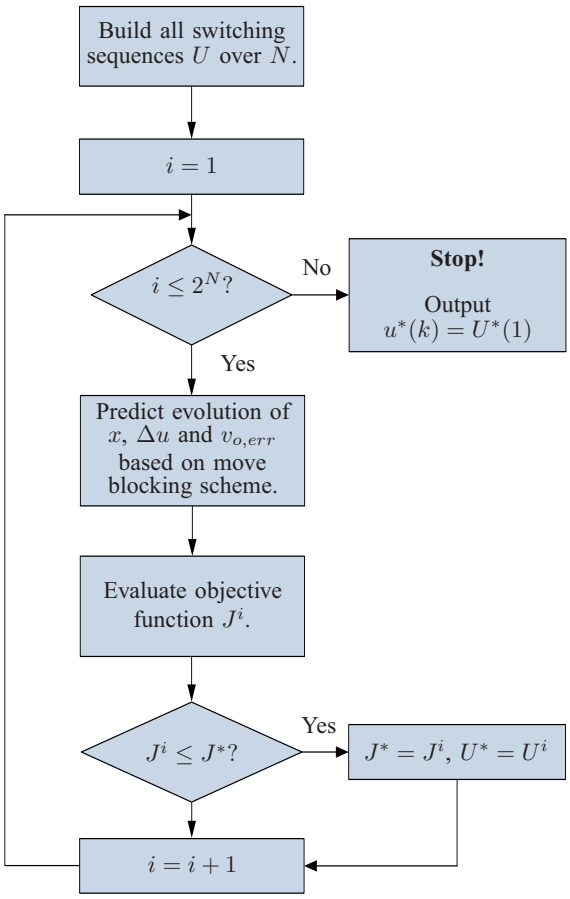

Fig. 4: Block diagram of the MPC algorithm.

If not otherwise stated, the input voltage is $v_s = 10\,\mathrm{V}$ and the reference of the output voltage is $v_{o,ref} = 15\,\mathrm{V}$. Finally, the covariance matrices of the Kalman filter are chosen as $Q = \mathrm{diag}(0.1, 0.1, 50, 50)$ and $R = \mathrm{diag}(1, 1)$.

A. Start-Up

The first case to be examined is that of the start-up behavior under nominal conditions. As can be seen in Fig. 5, the inductor current is very quickly increased until the capacitor is charged to the desired voltage level. The output voltage reaches its reference value in about $t \approx 1.8\,\mathrm{ms}$, without any noticeable overshoot. Subsequently, the converter operates in DCM with the inductor current reaching zero.

B. Step Change in the Output Reference Voltage

Next, a step change in the reference of the output voltage is considered. At time $t = 4\,\mathrm{ms}$ the reference is stepped up from $v_{o,ref} = 15\,\mathrm{V}$ to $v_{o,ref} = 30\,\mathrm{V}$. As can be seen in Fig. 6, the average current is increased to about 1.25 A to quickly ramp up the output voltage until it reaches its new reference value. The controller exhibits a satisfactory behavior during the transient, reaching the new output voltage in about $t \approx 2.5\,\mathrm{ms}$, without any overshoot.

C. Step Change in the Input Voltage

Operating at the previously attained steady-state operating point with $v_{o,ref} = 30\,\mathrm{V}$, the (measured) input voltage

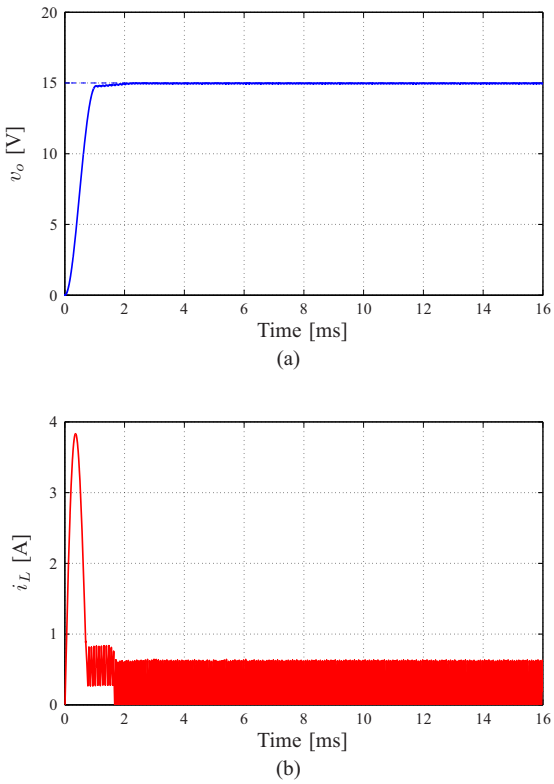

Fig. 5: Simulation results for nominal start-up: a) output voltage (solid line) and output voltage reference (dashed line), b) inductor current.

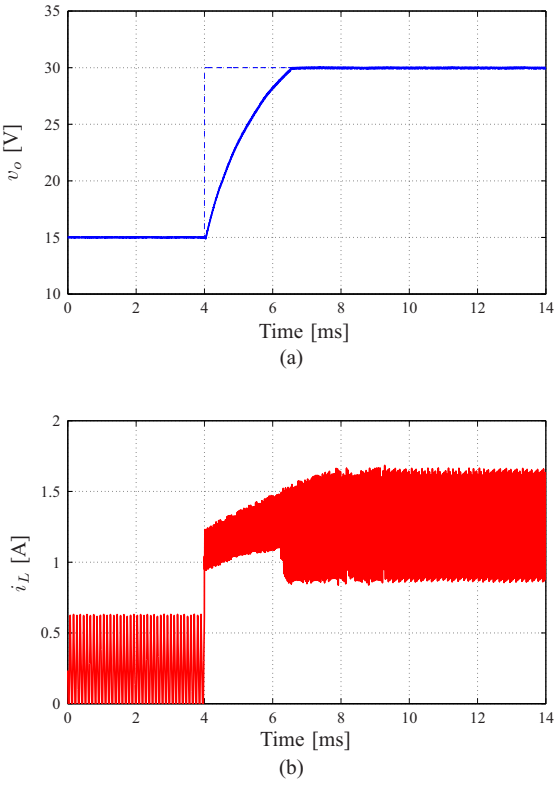

Fig. 6: Simulation results for a step-up change in the output voltage reference: a) output voltage (solid line) and output voltage reference (dashed line), b) inductor current.

is changed in a step-wise fashion. At time $t = 0.4\,\mathrm{ms}$ the

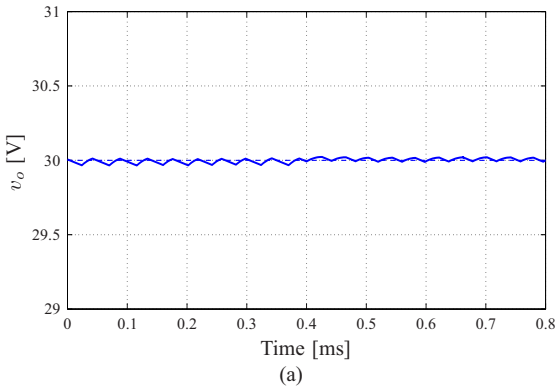

(a)

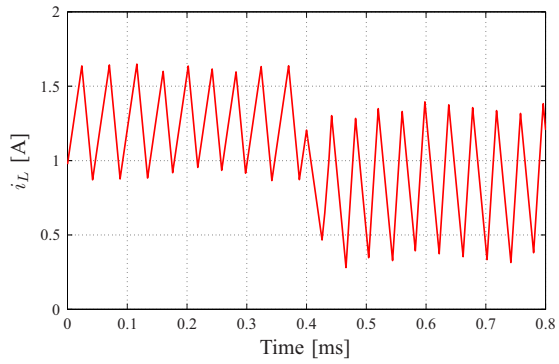

(b)

Fig. 7: Simulation results for a step-up change in the input voltage: a) output voltage (solid line) and output voltage reference (dashed line), b) inductor current.

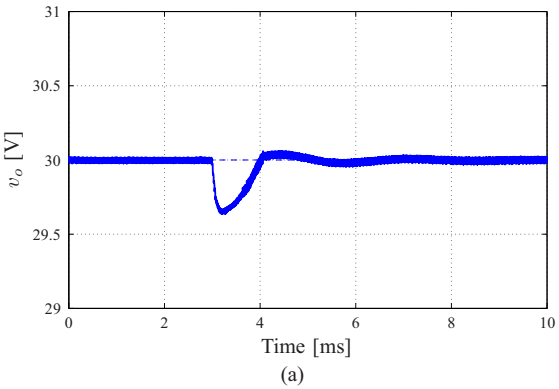

(a)

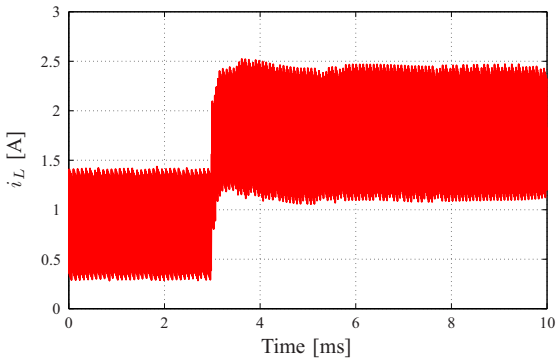

(b)

Fig. 8: Simulation results for a step-down change in the load: a) output voltage (solid line) and output voltage reference (dashed line), b) inductor current.

input voltage is increased from $v_s = 10\,\text{V}$ to $v_s = 15\,\text{V}$. The transient response of the converter is depicted in Fig. 7. The output voltage remains practically unaffected, with no undershoot observed, while the controller settles very quickly at the new steady-state operating point.

D. Load Step Change

The last case examined is that of a drop in the load resistance. As can be seen in Fig. 8, a step-down change in the load from $R = 73\,\Omega$ to $R = 36.5\,\Omega$ occurs at $t = 3\,\text{ms}$. The Kalman filter adjusts the output voltage reference to its new value so as to avoid any steady-state tracking error. This can be observed in Fig. 8(a); after the converter has settled at the new operating point, the output voltage accurately follows its reference.

VI. Experimental Validation

To further investigate the potential advantages of the proposed algorithm, the controller was implemented on a dSpace DS1104 real-time system. A boost converter was built using an IRF60 MOSFET and a MUR840 diode as active and passive switches, respectively. The values of the circuit elements are the same as in Section V. Moreover, the nominal input and output voltages and the nominal load resistance are the same as previously. The voltage and current measurements were obtained using Hall effect transducers.

Due to computational restrictions imposed by the computational platform, a six-step prediction horizon was implemented, i.e. $N = 6$ and the sampling interval was set to $T_s = 10\,\mu\text{s}$. The prediction horizon was split into $N_1 = 4$ and $N_2 = 2$ with $n_s = 2$. The weight in the objective function was chosen to be $\lambda = 0.5$. The covariance matrices of the Kalman filter are $Q = \text{diag}(0.1, 0.1, 50, 50)$ and $R = \text{diag}(1, 1)$.

A. Start-up

In Fig. 9 the output voltage and the inductor current of the converter are depicted during start-up. The inductor current rapidly increases to charge the output capacitor to the reference voltage level as fast as possible. The output voltage reaches its desired value in about $t \approx 2\,\text{ms}$.

B. Step Change in the Output Reference Voltage

The second case to be analyzed is that of the transient behavior during a step-up change in the output reference voltage from $v_{o,ref} = 15\,\text{V}$ to $v_{o,ref} = 30\,\text{V}$ at $t \approx 5.2\,\text{ms}$. The response of the converter is illustrated in Fig. 10. The inductor current instantaneously increases, enabling the output voltage to reach its new desired level as fast as possible. This happens in about $t \approx 2\,\text{ms}$, without a significant overshoot.

C. Ramp Change in the Input Voltage

Subsequently, the input voltage is manually increased from $v_s = 10\,\text{V}$ to $v_s = 15\,\text{V}$, resulting in a voltage ramp

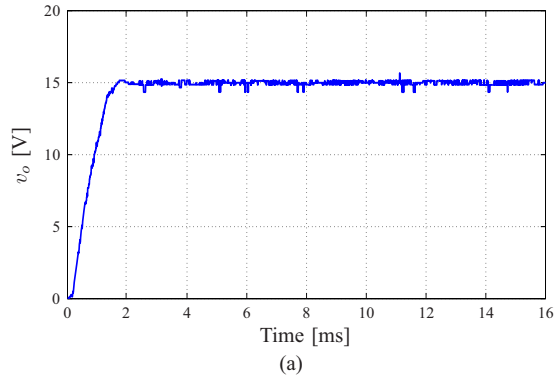

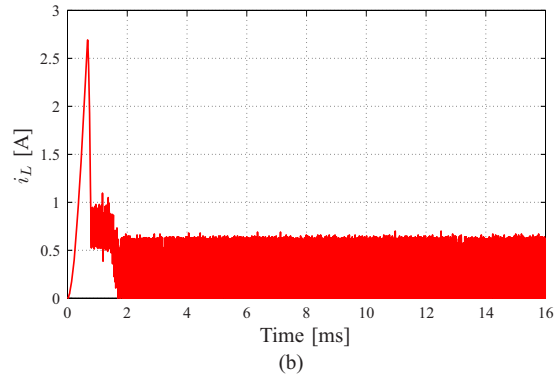

Fig. 9: Experimental results for nominal start-up: a) output voltage, and b) inductor current.

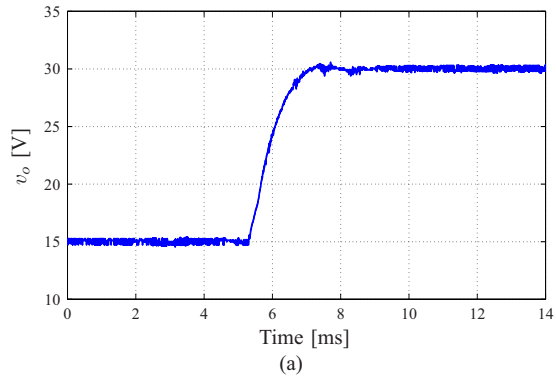

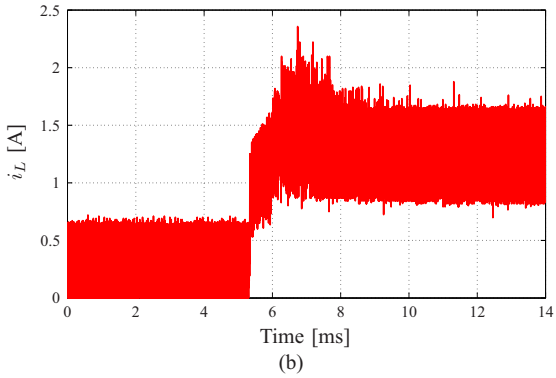

Fig. 10: Experimental results for a step-up change in the output voltage reference: a) output voltage, and b) inductor current.

from $t \approx 16\,\text{ms}$ until $t \approx 38\,\text{ms}$. During the transient,

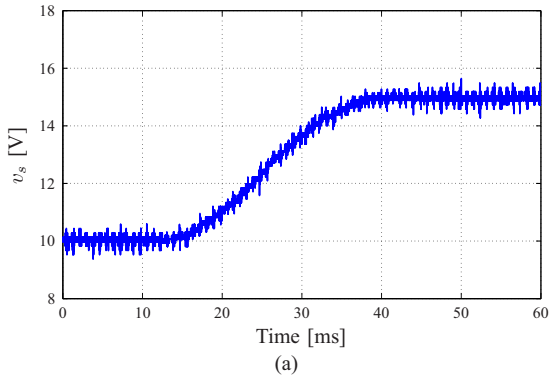

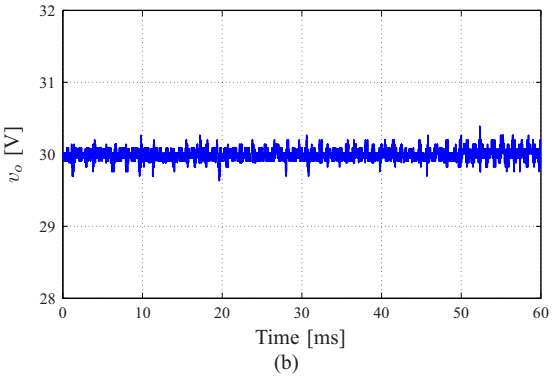

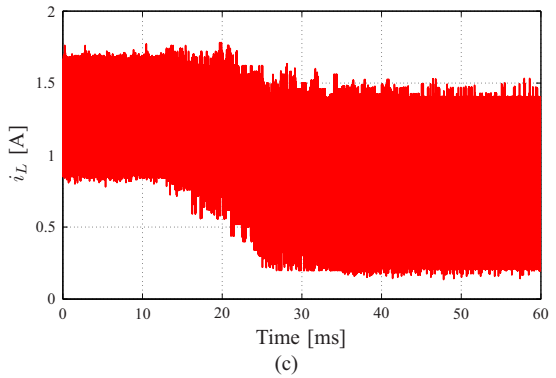

Fig. 11: Experimental results for a ramp change in the input voltage: a) input voltage, b) output voltage, and c) inductor current.

the inductor current changes accordingly in a ramp-like manner down to its new steady-state value. It can be seen that the output voltage remains unaffected and equal to its reference value, implying that input voltage disturbances are very effectively rejected by the controller and Kalman filter.

D. Load Step Change

The last case examined is that of a step-down change in the load resistance occurring at $t \approx 3.5\,\text{ms}$. With the converter operating at the previously attained operating point, the nominal load decreases by half, i.e. from $R = 73\,\Omega$ to $R = 36.5\,\Omega$. As can be observed in Fig. 12, the Kalman filter quickly adjusts the voltage reference, resulting in a zero steady-state error in the output voltage, thanks to its integrating nature.

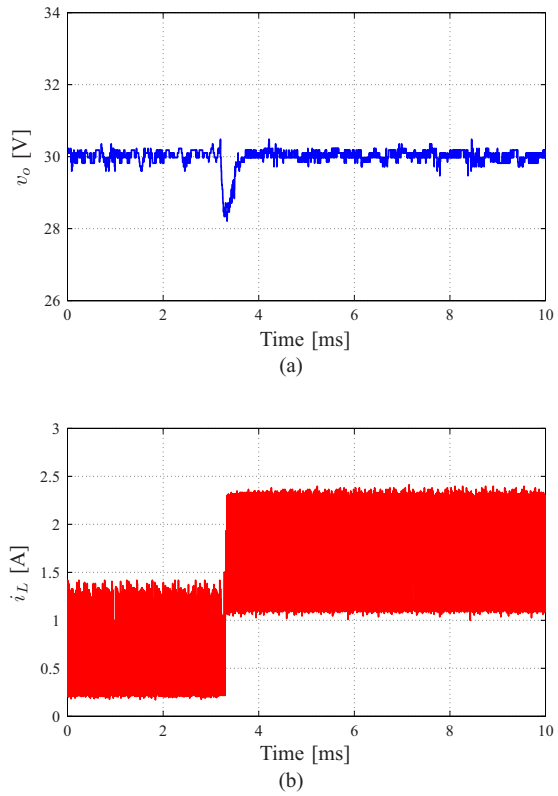

Fig. 12: Experimental results for a step change in the load: a) output voltage, and b) inductor current.

VII. Conclusion

A model predictive control approach based on enumeration for dc-dc boost converter is proposed that directly regulates the output voltage along its reference, without the use of a subsequent current control loop. This enables very fast dynamics during transients. Since the converter model is included in the controller, time-consuming tuning of controller gains is avoided. The computational complexity is somewhat pronounced, but significantly reduced by using a move blocking scheme. In addition to that, the switching frequency is variable. A load estimation scheme, namely a discrete-time switching Kalman filter, is implemented to allow for varying loads and robustness to parameter variations. Simulation and experimental results demonstrate the potential advantages of the proposed methodology.

References

[1] N. Mohan, T. M. Undeland, and W. P. Robbins, *Power Electronics: Converters, Applications and Design,* Wiley, 1989.

[2] D. Q. Mayne, J. B. Rawlings, C. V. Rao, and P. O. M. Scokaert, "Constrained model predictive control: Stability and optimality," *Automatica*, vol. 36, no. 6, pp. 789–814, Jun. 2000.

[3] T. Geyer, G. Papafotiou, and M. Morari, "Model predictive direct torque control—Part I: Concept, algorithm and analysis," *IEEE Trans. on Industrial Electronics,* vol. 56, no. 6, pp. 1894–1905, Jun. 2009.

[4] P. Cortés, M. P. Kazmierowski, R. M. Kennel, D. E. Quevedo, and J. Rodríguez, "Predictive control in power electronics and drives," *IEEE Trans. on Industrial Electronics*, vol. 55, no. 12, pp. 4312-4324, Dec. 2008.

[5] P. Cortés, J. Rodríguez, P. Antoniewicz, and M. Kazmierkowski, "Direct power control of an AFE using predictive control," *IEEE Trans. on Power Electronics*, vol. 23, no. 5, pp. 2516–2523, Sep. 2008.

[6] J. Chen, A. Prodic, R. W. Erickson, and D. Maksimovic, "Predictive digital current programmed control," *IEEE Trans. on Power Electronics*, vol. 18, no 1, pp. 411–419, Jan. 2003.

[7] F. M. Oettmeier, J. Neely, S. Pekarek, R. DeCarlo, and K. Uthaichana, "MPC of switching in a boost converter using a hybrid state model with a sliding mode observer," *IEEE Trans. on Industrial Electronics*, vol. 56, no. 9, pp. 3453–3466, Sep. 2009.

[8] T. Geyer, G. Papafotiou, R. Frasca, and M. Morari, "Constrained optimal control of the step-down DC-DC converter," *IEEE Trans. on Power Electronics*, vol. 23, no 5, pp. 2454–2464, Sep. 2008.

[9] A. G. Beccuti, G. Papafotiou, R. Frasca, and M. Morari, "Explicit hybrid model predictive control of the dc-dc boost converter," in *Proc. IEEE Power Electronics Specialist Conf. PESC*, Orlando, FL, USA, June 2007, pp. 2503–2509.

[10] A. G. Beccuti, S. Mariéthoz, S. Cliquennois, S. Wang, and M. Morari, "Explicit model predictive control of DC-DC switched-mode power supplies with extended Kalman filtering," *IEEE Trans. on Industrial Electronics*, vol. 56, no 6, pp. 1864–1874, June 2009.

[11] P. Karamanakos, G. Papafotiou, and S. Manias, "Model predictive control strategies for DC-DC boost voltage conversion," in *Proc. European Conf. on Power Electronics and Applications EPE*, Birmingham, UK, Aug./Sep. 2011, pp. 1–9.

[12] J. M. Maciejowski, *Predictive Control with Constraints,* Prentice Hall publications, 2002.

[13] J. B. Rawlings and D. Q. Mayne, *Model Predictive Control: Theory and Design,* Nob Hill Publ., 2009.

[14] R. W. Erickson, and D. Maksimovic, *Fundamentals of Power Electronics,* Kluwer Academic Publishers, 2nd edition, 2000.

[15] A. Bemporad, and M. Morari, "Control of systems integrating logic, dynamics, and constraints," *Automatica*, vol. 35, no. 3, pp. 407–427, Mar. 1999.

[16] T. Geyer, G. Papafotiou, and M. Morari, "Model predictive control in power electronics: A hybrid systems approach," in *Proc. IEEE Conf. on Decision and Control and European Control Conf. CDC-ECC*, Seville, Spain, Dec. 2005, pp. 5606–5611.

[17] G. Pannocchia, and J. B. Rawlings, "Disturbance models for offset-free model-predictive control," *AIChE Journal.*, vol. 49, no 2, pp. 426–437, Feb. 2003.